Eur. Phys. J. Spec. Top. (2026) 235:8019–8030
https://doi.org/10.1140/epjs/s11734-026-02410-y

THE EUROPEAN PHYSICAL JOURNAL SPECIAL TOPICS

Regular Article

Age-related EEG functional connectivity during visual search in children

Vladimir Antipov[1,a], Alexander Kuc[1], Oleg Piljugin[1], Marina Khramova[2], and Artem Badarin[1]

[1] Research Institute of Applied Artificial Intelligence and Digital Solutions, Plekhanov Russian University of Economics, 36 Stremyannyy Pereulok, Moscow 115054, Russia
[2] Higher School of Cybertechnologies, Mathematics and Statistics, Plekhanov Russian University of Economics, 36 Stremyannyy Pereulok, Moscow 115054, Russia

Received 16 April 2026 / Accepted 23 May 2026 / Published online 30 June 2026
© The Author(s), under exclusive licence to EDP Sciences, Springer-Verlag GmbH Germany, part of Springer Nature 2026

Abstract Understanding how functional brain networks reorganize during cognitive development is essential for characterizing the neural mechanisms underlying learning in children. This study investigates age-related differences in EEG functional connectivity during a visual search task in 95 school-age children aged 8–14 years, divided into three age groups. We used the imaginary part of coherency to estimate functional connectivity during visual search in the theta, alpha, and beta frequency bands. Network-based statistic analysis identified two frequency-specific subnetworks that distinguished the age groups: a theta-band subnetwork comprising interhemispheric frontal–central–temporal connections and a beta-band subnetwork comprising intrahemispheric temporal–central links. Connectivity strength in both subnetworks showed age-related increases that paralleled improvements in reaction time. Linear mixed-effects modeling further showed that subnetwork connectivity predicted visual search performance beyond the effects of age and task complexity. These findings suggest that age-related reorganization of frequency-specific brain networks may support developmental gains in visual search efficiency.

1 Introduction

The study of brain activity during cognitive tasks is essential for understanding the neural mechanisms that support learning and intellectual development in children [1]. Cognitive abilities such as attention, working memory, and executive control form the foundation of academic performance, and their level of development significantly influences the efficiency of the learning process [2, 3]. Among these abilities, visual search (the capacity to locate a target stimulus among distractors) occupies a prominent role, as it engages mechanisms of selective attention that are involved in a wide range of everyday and educational activities [4–6].

Visual search is closely related to executive functions through the mechanisms of cognitive control. According to the biased competition model, perception of visual scenes involves competition among multiple stimulus representations, and selective attention resolves this competition by applying top-down control signals that bias processing in favor of relevant targets [7]. These top-down attentional mechanisms undergo substantial maturation during childhood and adolescence, resulting in progressive improvements in search efficiency and accuracy [8]. Electrophysiological investigations of visual search in children have revealed that midfrontal theta synchronization and posterior alpha lateralization serve as markers of attentional processing, with their characteristics varying across developmental stages [9]. These findings suggest that the neural substrates of visual search are reorganized with age, yet the network-level mechanisms underlying this reorganization remain insufficiently understood.

A growing body of evidence suggests that the developing brain can be viewed as a self-organizing system, in which functional networks progressively emerge, reorganize, and stabilize through recurrent interactions among neural activity, maturation, and experience [10, 11]. During childhood, EEG-based network analysis has revealed a shift from more random to more structured small-world topologies, consistent with the formation of increasingly efficient communication architectures [11]. In parallel, recent advances in complex network science indicate that neural dynamics cannot always be fully captured by pairwise connectivity measures alone, since higher order

[a] e-mail: vantipovm@gmail.com (corresponding author)

interactions involving three or more regions may contribute to collective neural activity and emergent cognitive functions [12–14]. Such network approaches have proven fruitful not only in neuroscience but also in mapping research trends in AI-driven medicine [15]. These perspectives suggest that developmental changes in the brain networks supporting visual search should be understood not merely as a strengthening of isolated connections, but as an age-related reorganization of task-relevant functional architectures [16].

Electroencephalography (EEG) has proven to be an effective tool for investigating age-related changes in brain activity, owing to its high temporal resolution and applicability in near-natural experimental settings [17, 18]. EEG studies of oscillatory activity have demonstrated systematic developmental trends: the dominant posterior rhythm shifts from the theta to the alpha frequency range at approximately 7–8 years of age [19], the aperiodic spectral slope flattens progressively throughout childhood [20], and task-related theta and alpha responses become increasingly differentiated with maturation [21, 22]. However, spectral power analysis reflects the activity of individual brain regions and does not capture the coordinated interactions between spatially distributed neural populations that give rise to complex cognitive functions, including visual attention [23].

This limitation motivates the application of functional connectivity analysis, which quantifies statistical dependencies between signals recorded at different scalp locations and thereby reveals the organization and topology of brain networks [24, 25]. Studies of EEG coherence have shown that functional connectivity in children develops systematically with age, with increasing coupling observed predominantly in long-range intrahemispheric and interhemispheric electrode pairs [26]. This progressive strengthening of inter-regional interactions has been associated with the maturation and restructuring of large-scale functional networks [27, 28]. Importantly, not only resting-state but also task-evoked connectivity patterns exhibit age-dependent reorganization during attentional processing [29], indicating that network analysis during cognitively demanding tasks provides complementary information about brain development [30].

A well-known methodological concern in EEG connectivity estimation is the effect of volume conduction, whereby a single cortical source projects simultaneously to multiple electrodes, producing spurious zero-phase-lag correlations that do not reflect genuine neural interactions. To address this problem, the imaginary part of coherency (ImCoh) was proposed as a connectivity measure that is strictly insensitive to instantaneous signal mixing [31]. Volume conduction contributes exclusively to the real part of the cross-spectrum, while the imaginary component captures only interactions with a non-zero time delay that cannot be explained by field spread. This property makes ImCoh a robust tool for investigating genuine functional coupling, and it has been successfully applied in developmental populations, including studies of connectivity alterations in children with autism spectrum disorder [32–34]. Further methodological refinements have been proposed to extend the capabilities of this approach [35].

Despite considerable progress in understanding developmental changes in brain connectivity, several gaps persist. The majority of existing studies have examined resting-state connectivity, while task-related network reorganization during specific cognitive operations has received less attention. In particular, the network-level mechanisms underlying visual search have not been systematically investigated across age groups in school-age children. Furthermore, most developmental studies have relied on conventional coherence measures without controlling for volume conduction artifacts. The age range of 8–14 years is of special interest in this context, as it encompasses a period of intensive maturation of frontoparietal attention networks and executive control systems [8, 27, 29], yet comparisons between closely spaced age groups within this range remain scarce. From the perspective of self-organization, it remains an open question how the functional networks that support visual search spontaneously emerge and consolidate during this critical developmental window, and whether their formation follows frequency-specific organizational principles.

Our previous work [36] showed that the combination of behavioral and neurophysiological characteristics obtained during cognitive testing allows evaluating the level of development of individual cognitive abilities. Based on these results, the present study is aimed at investigating the relationship between the efficiency of visual search task performance and the functional connectivity of neural activity clusters across different age groups of students. We frame this investigation within the context of self-organization in complex brain networks, asking how task-relevant functional architectures emerge and reorganize with age. We employ ImCoh to analyze functional brain network interactions during visual search across theta, alpha, and beta frequency bands, and examine how the topology of functional connectivity patterns is reorganized with age.

2 Materials and methods

2.1 Experimental procedure

The experimental paradigm employed in this study was based on the visual search assessment test developed and validated in our previous work [36]. The visual search task was designed to evaluate the participant's ability to locate a target stimulus among distractors, engaging mechanisms of selective visual attention and cognitive control.

The structure of a single trial is illustrated in Fig. 1. Each trial began with the presentation of a fixation cross at

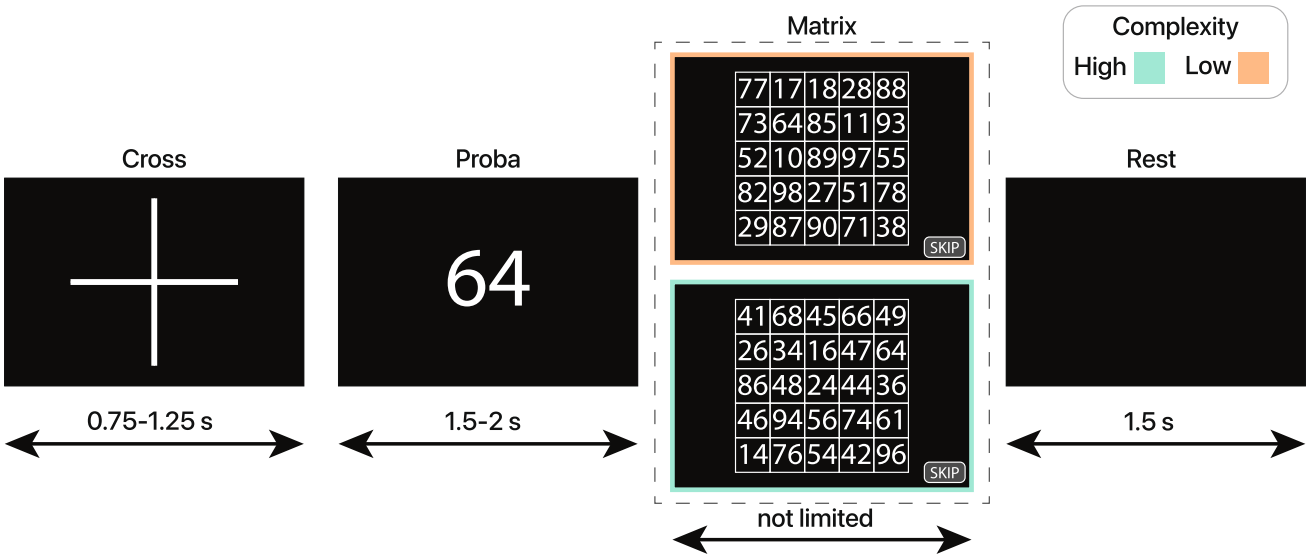


Fig. 1 Design of the visual search task. A fixation cross is followed by a two-digit target number (probe) and a 5×5 matrix of two-digit numbers in which the participant must locate the target. Orange and cyan borders indicate low-complexity and high-complexity matrices, respectively

the center of the screen for a randomized duration of 0.75–1.25 s. The variable duration of the fixation cross was employed to prevent temporal anticipation and habituation effects [36]. Following the fixation cross, a two-digit target number (probe) was displayed on the screen for 1.5–2.0 s. The participant was instructed to memorize this number.

After the probe disappeared, a 5×5 matrix containing 25 two-digit numbers was presented. The participant's task was to locate the target number within the matrix and indicate it by pressing the corresponding cell on the touchscreen. The matrix remained visible until the participant provided a response. Additionally, a "SKIP" button was available, allowing the participant to skip the current trial if they were unable to recall the target number. After the participant's response, a rest interval of 1.5 s followed before the next trial commenced.

To manipulate task difficulty, two types of matrices were used, corresponding to two levels of complexity (Fig. 1). In low-complexity trials, the distractor numbers in the matrix did not contain any of the digits present in the target number. For example, if the target number was 64, the distractors would consist of numbers such as 17, 89, 30, and 55. In high-complexity trials, the distractor numbers shared at least one digit with the target number (e.g., for the target 64, the distractors could include 46, 61, 74, and 34), thereby increasing the perceptual similarity between the target and distractors and requiring more effortful visual discrimination. This manipulation was introduced to assess visual search performance under conditions of varying target–distractor similarity [36]. The test uses equal number of tables of the first and the second type, randomly mixed. There are 10 tasks for each type of table, resulting in a total of 20 tasks.

All stimuli were presented using a custom-developed electronic environment running on a touchscreen device (14-inch diagonal, 1920×1080 resolution) positioned at a viewing distance of approximately 30 cm. Prior to the main experiment, participants completed a familiarization phase, during which the researcher explained the task instructions and the participant performed several practice trials to ensure comprehension of the procedure.

2.2 Participants

The study involved 95 children, all pupils from the same school, divided into three age groups: Group 1 ($n = 24$, 14 boys and 10 girls, mean age $= 9.5 \pm 0.7$ years, grades 3–4), Group 2 ($n = 28$, 17 boys and 11 girls, mean age $= 11.3 \pm 0.6$ years, grade 5), and Group 3 ($n = 43$, 22 boys and 21 girls, mean age $= 13.1 \pm 0.4$ years, grade 7). All participants had normal or corrected-to-normal vision. None of the participants had a diagnosed central nervous system disorder.

All experiments were conducted in the first half of the day. The study was conducted in accordance with the Declaration of Helsinki and approved by the local ethics committee. Prior to the experiment, participants were informed about the study's objectives and methods. Written informed consent was obtained from the parents or legal guardians of each participant.

2.3 Data acquisition and preprocessing

EEG signals were recorded using the LiveAmp amplifier (Brain Products, Germany), a compact wearable device suitable for use in near-natural experimental settings. The recording was performed from 64 scalp electrodes at a sampling rate of 500 Hz. Electrodes were positioned according to the international "10–10" system, with the ground electrode placed at Fpz and the reference electrode at Fz. Prior to electrode placement, the scalp was prepared with NuPrep abrasive gel to reduce skin impedance, and SuperVisc conductive gel was applied to each electrode to ensure impedance values below 10 kΩ and high signal quality throughout the recording session.

2.3.1 EEG preprocessing

EEG data preprocessing was performed using the MNE-Python library [37]. First, a bandpass filter (1–40 Hz) was applied to remove low-frequency drift and high-frequency artifacts. Second, independent component analysis (ICA) based on the FastICA algorithm with 64 components was used to identify and remove ocular artifacts [38]. Artifact-related components were visually inspected and excluded, and clean EEG signals were reconstructed from the remaining components. Epochs were then rejected based on a peak-to-peak amplitude threshold of 150 μV.

2.3.2 Functional connectivity estimation

To quantify functional connectivity between EEG channels, we computed the ImCoh, a measure specifically designed to be insensitive to spurious zero-phase-lag correlations arising from volume conduction [31]. Given two EEG signals $x_i(t)$ and $x_j(t)$ with Fourier transforms $x_i(f)$ and $x_j(f)$, the cross-spectrum is defined as

$$S_{ij}(f) = \langle x_i(f)\, x_j^*(f) \rangle, \tag{1}$$

where * denotes complex conjugation and $\langle \cdot \rangle$ indicates the expectation value estimated by averaging over epochs. The complex-valued coherency is obtained by normalizing the cross-spectrum:

$$C_{ij}(f) = \frac{S_{ij}(f)}{\sqrt{S_{ii}(f)\, S_{jj}(f)}}. \tag{2}$$

Under the quasi-static approximation, the mapping from brain sources to scalp electrodes is instantaneous, and therefore, the cross-spectrum of non-interacting sources is strictly real-valued [31]. Consequently, a non-vanishing ImCoh $\mathrm{Im}(C_{ij}(f))$ can only arise from genuine neural interactions involving a non-zero time lag, making this measure robust against volume conduction artifacts.

ImCoh was computed using the multitaper spectral estimation method within the MNE-Connectivity framework in Python with adaptive weighting and tapers exceeding 90% spectral concentration. For each trial, connectivity was estimated over all unique electrode pairs within a time window extending from the onset of the search matrix presentation to the participant's response and averaged within three frequency bands of interest. Trials with "SKIP" responses were excluded from the analysis. These connectivity estimates were used for subsequent analyses of age-related and task-related differences.

The frequency bands were defined as theta (2.5–7.5 Hz), alpha (7.5–13.5 Hz), and beta (13.5–20.5 Hz). These boundaries were shifted toward lower frequencies compared to the conventional adult definitions to account for the well-documented developmental deceleration of the peak alpha frequency in school-age children. During this period, the dominant posterior rhythm progressively increases from approximately 6–8 Hz in younger children to adult-like values of 9–11 Hz by mid-adolescence [19, 39]. The adjusted frequency ranges employed in this study were selected to more accurately capture the dominant oscillatory activity within each band for the age groups under investigation.

2.3.3 Statistical analysis of network connectivity

To identify differences in network connectivity across the three experimental groups, we employed the network-based statistic (NBS) approach [40]. The NBS is a method specifically designed to control the family-wise error rate when conducting mass-univariate testing across all connections in a brain network, while exploiting the inherent interconnectedness of the data to enhance statistical power. Grounded in the principles of cluster-based thresholding used in traditional neuroimaging analyses, the NBS identifies sets of connections that form connected components within the network and evaluates their significance against a null distribution derived from nonparametric permutation testing.

The analysis was performed using a general linear model (GLM) framework. A design matrix was constructed to model group membership, with three categorical predictors representing the three grade groups. A contrast vector was specified to test for the main effect of group, assessing whether connectivity strength varied systematically across the three groups. For each of the unique connections (edges) in the network, an F-statistic was computed to quantify the between-group difference.

The NBS procedure was then applied as follows. First, a primary threshold was applied to the F-statistic map, retaining only those connections whose test statistic exceeded a predefined value. This thresholded set of connections was treated as a graph, within which all connected components were identified using graph-theoretic algorithms. The size of each component was quantified using an intensity-based measure, defined as the sum of the F-statistics of all connections comprising the component. This component size served as the test statistic for the NBS.

To obtain the null distribution of component sizes, a nonparametric permutation strategy was implemented. The group labels were randomly permuted 10,000 times, preserving the exchangeability structure of the data. For each permutation, the GLM was re-estimated, the same primary threshold was applied, and the size of the largest connected component was recorded. This process generated an empirical null distribution of maximal component sizes under the null hypothesis of no group differences. For each component identified in the original, unpermuted data, its observed intensity-based size was compared against this null distribution, and a corrected p-value was calculated as the proportion of permutations in which the maximal component size equaled or exceeded the observed component size. Components with a corrected p-value below the significance threshold ($\alpha = 0.05$) were considered statistically significant.

This approach allowed for the identification of subnetworks (interconnected sets of EEG channels) exhibiting significant differences in functional connectivity across the three grade groups. By evaluating significance at the level of entire components rather than individual connections, the NBS provided enhanced power to detect cohesive, topologically structured effects while maintaining stringent control over the family-wise error rate. All computations were performed using custom software implementing the NBS within the MATLAB environment. The primary F-statistic threshold was set to 5.

2.3.4 Network characterization within significant subnetworks

To characterize functional connectivity within the subnetworks identified by the NBS analysis, we computed the mean connection weight for each participant and trial. For each frequency band (theta and beta), a binary mask corresponding to the significant NBS component was applied to the individual ImCoh connectivity matrix. The mean connection weight was then calculated as the average of the absolute ImCoh values across all edges belonging to the identified subnetwork:

$$\bar{w} = \frac{1}{|E|} \sum_{(i,j)\in E} |\mathrm{Im}(C_{ij})|, \tag{3}$$

where E denotes the set of edges in the significant NBS component and $|E|$ is the number of such edges. These values were then submitted to a repeated-measures analysis of variance (RM-ANOVA) with age group as a between-subjects factor and task complexity as a within-subjects factor.

2.3.5 Linear mixed-effects modeling of reaction time

To test whether functional connectivity within the identified NBS subnetworks explained visual search performance beyond the effects of age and task complexity, we fitted a series of linear mixed-effects models [41] with log-transformed reaction time (ln(RT)) as the dependent variable. Log transformation was applied to reduce the positive skewness of the reaction time distribution, as commonly recommended for response latency data [42].

All models included subject-specific random intercepts to account for repeated measurements within participants. Fixed effects were built incrementally across four nested models: Model 1 included age group and task complexity as predictors; Model 2 additionally included the mean connection weight in the theta-band NBS subnetwork ($\bar{w}_\theta$); Model 3 instead added the mean connection weight in the beta-band subnetwork ($\bar{w}_\beta$); and Model 4 included both connectivity predictors simultaneously. Models were estimated using restricted maximum likelihood (REML) with the Powell optimization method, as implemented in the `statsmodels` library in Python. Statistical significance of fixed effects was assessed using Wald z-tests, with effects considered significant at $p < 0.05$. Model comparison was performed using the Akaike Information Criterion (AIC) and Bayesian Information Criterion (BIC) computed under maximum likelihood estimation.

3 Results

To characterize age-related differences in visual search performance, we analyzed log-transformed reaction times using a mixed ANOVA with age group (Group 1, Group 2, Group 3) as a between-subjects factor and task complexity (high, low) as a within-subjects factor. The analysis revealed a significant main effect of age group ($F(2, 92) = 27.26$, $p < 0.001$, $\eta_p^2 = .372$) and a significant main effect of complexity ($F(1, 92) = 132.29$, $p < 0.001$, $\eta_p^2 = .590$), while the interaction between these factors was not significant ($F(2, 92) = 0.42$, $p = 0.655$).

As shown in Fig. 2, reaction times decreased with age across both complexity conditions. Post-hoc pairwise comparisons using Welch's t-test with Holm correction (Table 1) indicated that Group 1 responded significantly slower than both Group 2 ($p < 0.001$) and Group 3 ($p < 0.001$), whereas the difference between Group 2 and Group 3 was not significant ($p = 0.191$).

These results indicate a marked decrease in reaction time from Group 1 to Group 2, with no significant difference between Group 2 and Group 3. Additionally, high-complexity trials elicited significantly longer reaction times than low-complexity trials across all age groups (Table 2), confirming that increased target–distractor similarity imposed greater demands on attentional selection.

The observed behavioral pattern is consistent with the known trajectory of attentional development during middle childhood. The sharp improvement between Group 1 and Group 2 likely reflects the maturation of top-down attentional control mechanisms, while the absence of further gains between Group 2 and Group 3 suggests

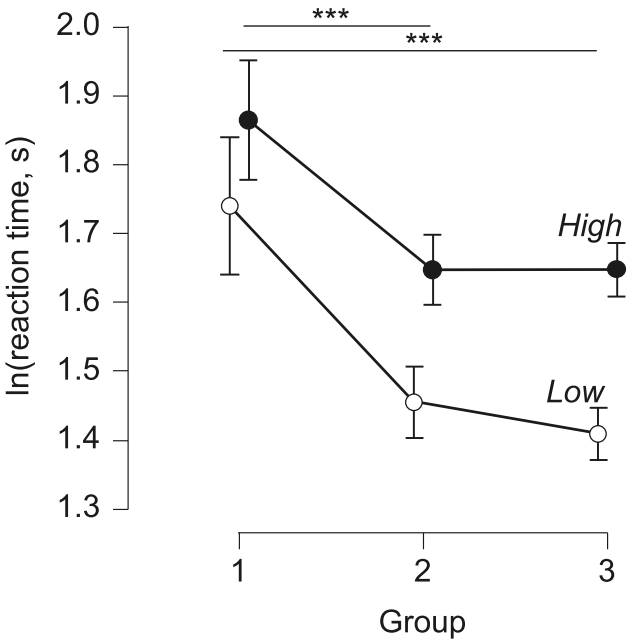


Fig. 2 Log-transformed reaction time across the three age groups for high-complexity and low-complexity visual search trials. Error bars represent the 95% confidence interval. Horizontal brackets with asterisks indicate statistically significant pairwise differences between groups ($^{***}p < 0.001$)

Table 1 Post-hoc pairwise comparisons between age groups for log-transformed reaction time (Welch's t-test)

		Mean difference	SE	df	t	p_{holm}
Group 1	Group 2	0.259	0.045	49.1	5.802	< .001
	Group 3	0.314	0.043	53.1	7.359	< .001
Group 2	Group 3	0.055	0.041	62.2	1.322	.191

P-values are adjusted using the Holm method. Results are averaged across all levels of complexity

Table 2 Post-hoc pairwise comparison between complexity levels for log-transformed reaction time (paired t-test)

		Mean difference	SE	df	t	p_{holm}
High	Low	0.242	0.021	94	11.573	< .001

Results are averaged across all levels of age group

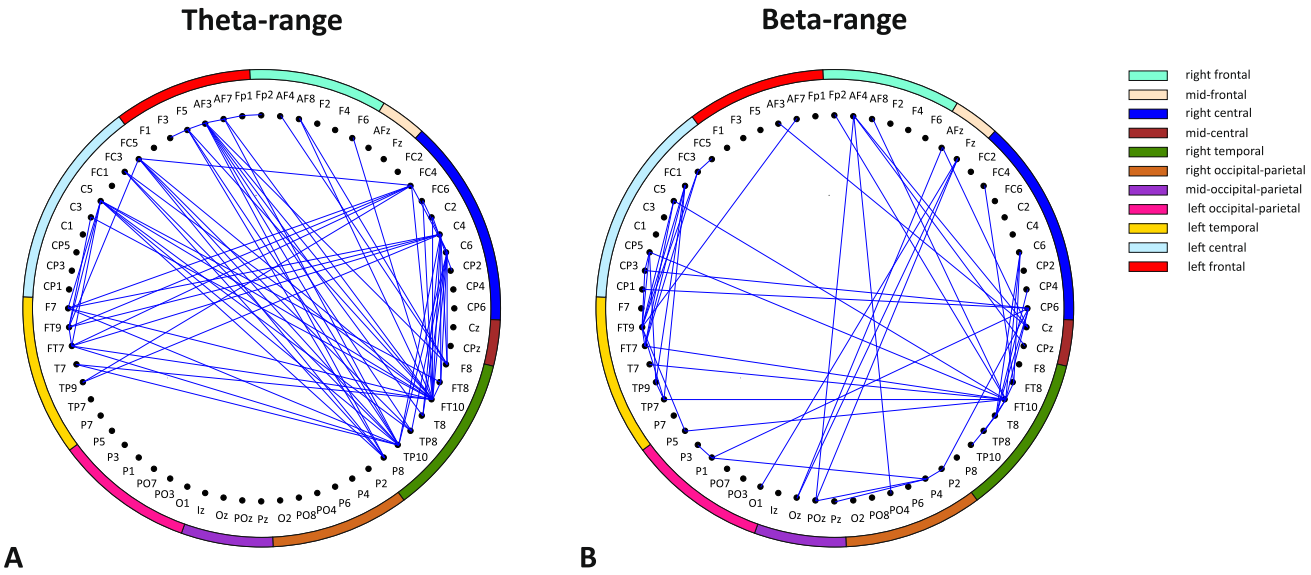


Fig. 3 Statistically significant functional connectivity subnetworks identified via network-based statistic (NBS) analysis for theta (A) and beta (B) frequency ranges. Nodes represent EEG electrodes, with color coding denoting anatomical regions. Significant connections ($p < 0.05$) are illustrated as blue lines

that the core mechanisms of visual search reach a relatively stable level of efficiency by approximately 11–12 years of age.

Next, we examined whether these behavioral gains are accompanied by reorganization of functional brain networks (Fig. 3). To this end, we applied the NBS to the ImCoh connectivity matrices obtained during the visual search task, testing for differences across the three age groups in the theta, alpha, and beta frequency bands.

NBS analysis revealed significant differences in functional connectivity patterns across the three groups within the theta and beta frequency bands, while no significant effects were observed in the alpha band.

In the theta frequency range, a statistically significant connected component was identified ($p = 0.036$), characterized by a distributed network of interhemispheric connections spanning left frontal, central, and temporal regions, as well as right frontal, central, and temporal areas. This subnetwork reflected coordinated interactions between the right and left hemispheres in the anterior and central regions of the cerebral cortex, indicating large-scale interhemispheric integration.

The beta frequency range demonstrated a distinct pattern of significant connectivity differences ($p = 0.022$), with a localized subnetwork centered on temporal and central regions. This configuration exhibited pronounced intrahemispheric connectivity, particularly between temporal and central regions.

These findings indicate that developmental variations in functional brain network organization are frequency-specific, with theta-band connectivity reflecting large-scale interhemispheric integration and beta-band connectivity emphasizing localized, within-hemisphere coordination across the studied age groups.

To further quantify the age-related differences within the identified subnetworks, we computed the mean connection weight ($\bar{w}$) for each participant and submitted these values to a mixed ANOVA with age group as a between-subjects factor and task complexity as a within-subjects factor. In the beta band, a significant main effect of age group was observed ($F(2, 92) = 12.64$, $p < 0.001$), while neither the effect of complexity ($F(1, 92) = 0.017$, $p = 0.896$) nor the group-by-complexity interaction ($F(2, 92) = 1.00$, $p = 0.373$) reached significance. A similar pattern emerged in the theta band: the main effect of age group was significant ($F(2, 92) = 5.81$, $p = 0.004$), with no significant effect of complexity ($F(1, 92) = 1.08$, $p = 0.301$) or interaction ($F(2, 92) = 2.15$, $p = 0.123$). These results indicate that connectivity strength within both subnetworks varied systematically across age groups but was not modulated by task difficulty.

Post-hoc pairwise comparisons revealed that in both frequency bands, Group 1 exhibited significantly lower mean connection weight compared to Group 2 and Group 3 ($p < 0.001$), whereas Group 2 and Group 3 did not differ significantly from each other (Fig. 4). This developmental pattern mirrors the behavioral results, where the most pronounced improvement in reaction time was also observed between Group 1 and Group 2, with a subsequent plateau. Notably, the absence of a complexity effect on $\bar{w}$ in either frequency band suggests that the identified subnetworks reflect stable, trait-like features of brain network organization that characterize a given developmental stage, rather than transient modulations driven by momentary task demands.

Having established that the NBS analysis revealed frequency-specific subnetworks with significant age-related differences in functional connectivity, we next sought to determine whether these connectivity patterns were

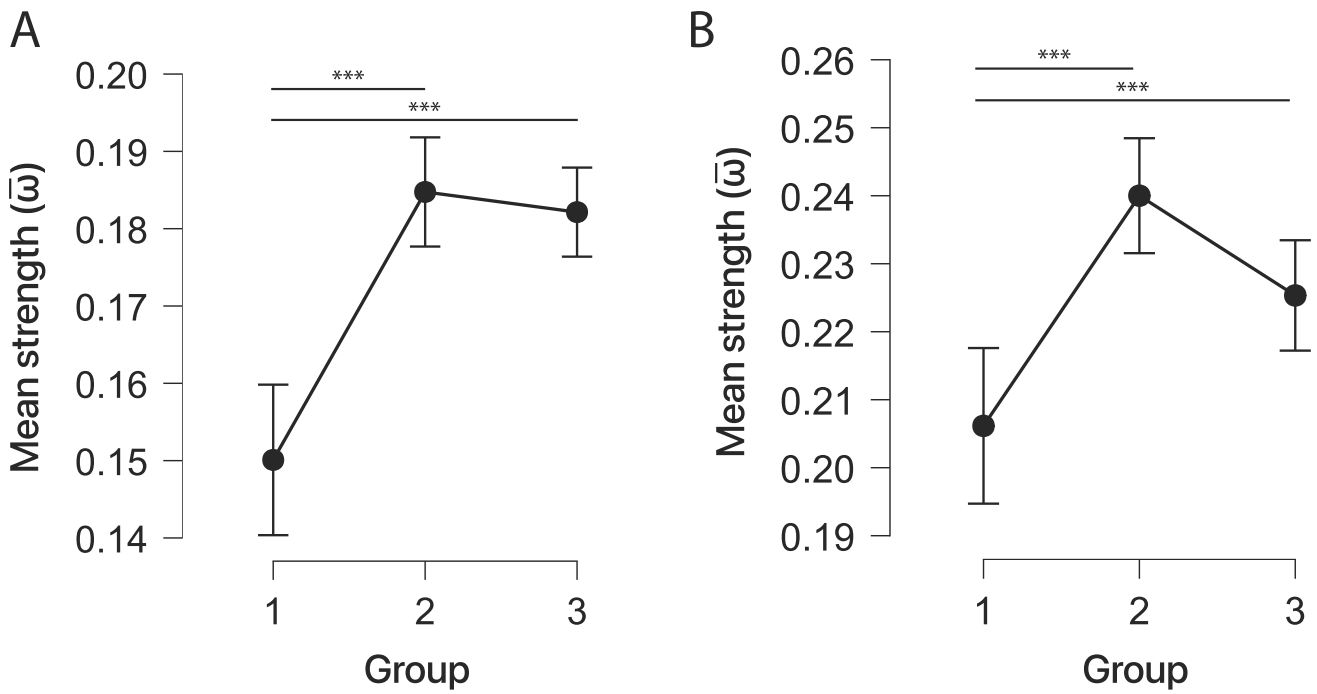


Fig. 4 Mean connection weight ($\bar{w}$) within the significant NBS subnetworks across the three age groups for the theta (A) and beta (B) frequency bands. Error bars represent the 95% confidence interval. Horizontal brackets with asterisks indicate statistically significant pairwise differences between groups ($^{***}p < 0.001$)

functionally relevant, i.e., whether they predicted actual visual search performance. This analysis was motivated by the central aim of the present study—to investigate the relationship between the efficiency of visual search task performance and the functional connectivity of neural activity clusters across different age groups [36]. Specifically, we tested whether the mean connection weight within the identified theta- and beta-band subnetworks contributed to explaining trial-level reaction time variability beyond what could be accounted for by age group and task complexity alone. To this end, we compared four nested linear mixed-effects models (Table 3).

In Model 1, both age group and task complexity were significant predictors of log-transformed reaction time. Older children responded faster than the youngest group (Group 2: $\beta = -0.263$, $p < 0.001$; Group 3: $\beta = -0.311$, $p < 0.001$), and low-complexity trials were associated with shorter reaction times ($\beta = -0.238$, $p < 0.001$).

Adding the mean connection weight within the theta-band NBS subnetwork (Model 2) significantly improved model fit ($\Delta\text{AIC} = -10.5$). Stronger theta-band connectivity was associated with faster responses ($\beta = -0.835$, $p < 0.001$). A comparable improvement was observed when the beta-band connectivity predictor was included instead (Model 3: $\beta = -0.943$, $p = 0.001$; $\Delta\text{AIC} = -8.9$). The full model incorporating both predictors (Model 4) yielded the lowest AIC value (10,110.0), with both theta ($\beta = -0.648$, $p = 0.010$) and beta ($\beta = -0.682$, $p = 0.025$)

Table 3 Fixed-effect estimates from linear mixed-effects models predicting log-transformed reaction time

Predictor	Model 1	Model 2	Model 3	Model 4
Intercept	1.797^{***}	1.875^{***}	1.879^{***}	1.916^{***}
Group 2 vs. 1	-0.263^{***}	-0.251^{***}	-0.245^{***}	-0.240^{***}
Group 3 vs. 1	-0.311^{***}	-0.304^{***}	-0.294^{***}	-0.293^{***}
Complexity	-0.238^{***}	-0.238^{***}	-0.238^{***}	-0.238^{***}
$\bar{w}_\theta$	–	-0.835^{***}	–	-0.648^{*}
$\bar{w}_\beta$	–	–	-0.943^{**}	-0.682^{*}
AIC	10,123.6	10,113.1	10,114.7	10,110.0
BIC	10,163.2	10,159.3	10,160.9	10,162.8

Model 1 includes group and complexity; Models 2–4 additionally include mean connection weight within the theta ($\bar{w}_\theta$) and/or beta ($\bar{w}_\beta$) NBS subnetworks. $^{*}p < 0.05$, $^{**}p < 0.01$, $^{***}p < 0.001$

connectivity retaining significance. Notably, the effect of age group was attenuated but remained significant in all models, suggesting that functional connectivity partially mediates the relationship between age and visual search performance.

4 Discussion

This study examined age-related differences in EEG functional connectivity during visual search in school-age children aged 8 to 14 years. The main objective was to identify frequency-specific patterns of brain network reorganization across three age groups and to determine whether task connectivity predicted behavioral performance. Using the ImCoh, which is robust to volume conduction artifacts [31], we identified significant developmental differences in theta- and beta-band subnetworks, while no effects were observed in the alpha band.

The behavioral results revealed a significant decrease in reaction time between Group 1 and Groups 2–3, with no further improvement between Groups 2 and 3. This nonlinear developmental trajectory is consistent with recent findings showing that executive attention and cognitive control undergo rapid maturation during late childhood, reaching a relative plateau by early adolescence [43]. The absence of a significant group-by-complexity interaction suggests that the age-related improvement reflects a general increase in processing speed rather than a selective enhancement of the ability to resolve target–distractor competition.

The NBS analysis revealed that theta-band connectivity differences were characterized by a distributed interhemispheric subnetwork connecting frontal, central, and temporal regions. This finding aligns with evidence that frontal theta oscillations support cognitive control and attentional coordination through long-range synchronization [44, 45]. In the context of visual search, theta-band interhemispheric coupling may reflect the coordination of top-down attentional signals across hemispheres, a process known to mature substantially during the age range studied here. The distributed, interhemispheric topology of this theta subnetwork is consistent with the self-organizing principle of integration, whereby long-range connections between distant cortical regions emerge during development to support coordinated cognitive processing [11].

In contrast, the beta-band subnetwork exhibiting significant group differences was more localized, centered on temporal and central regions with a predominantly intrahemispheric topology. Beta oscillations have been associated with the maintenance of sensorimotor representations and feedback-driven processing in visual perception [46, 47]. The intrahemispheric pattern observed here may reflect the maturation of local processing circuits involved in perceptual discrimination, which is consistent with the known role of beta synchronization in maintaining current cognitive set during visual tasks [48]. The increased beta-band connectivity in older children may indicate more efficient local information transfer supporting target identification within the visual search matrix.

The absence of significant age-related differences in the alpha band was unexpected, given that alpha oscillations are well-established markers of visual attention [49]. One possible explanation relates to the frequency band definitions used in this study. We adjusted the band boundaries toward lower frequencies (theta: 2.5–7.5 Hz, alpha: 7.5–13.5 Hz, beta: 13.5–20.5 Hz) to account for the developmental deceleration of the peak alpha frequency in younger children [19]. However, this single set of boundaries may not have been equally appropriate for all three age groups. In older children (Group 3), the individual alpha frequency approaches adult values of 10–11 Hz [50], and the adjusted band may have captured a mixture of slow alpha and residual theta activity, diluting any genuine connectivity effects. Future studies could address this limitation by employing individual alpha frequency estimation to define subject-specific frequency bands, an approach that has been shown to improve the sensitivity of oscillatory analyses in developmental populations [49].

A key finding of this study is that functional connectivity within the identified subnetworks predicted visual search performance beyond the effects of age and task complexity. The linear mixed-effects models demonstrated that both theta- and beta-band connectivity independently contributed to explaining reaction time variability, with the full model yielding the lowest AIC, although BIC marginally favored the more parsimonious Model 2 containing only theta-band connectivity. The negative association between connectivity strength and reaction time suggests that children with stronger task-related coupling within these subnetworks tended to perform visual search more efficiently. Importantly, the partial attenuation of the age group effect upon inclusion of connectivity predictors suggests that network maturation partially mediates the relationship between age and cognitive performance [51]. This finding extends previous work linking EEG connectivity to cognitive development by demonstrating that frequency-specific task-evoked networks carry behaviorally relevant information in a visual search context [43].

The present study has several limitations. First, the sample sizes across groups were unequal, with Group 3 being the largest, which may affect the statistical power of between-group comparisons. Second, the cross-sectional design does not permit causal inferences about the directionality of brain–behavior relationships; longitudinal studies are needed to track individual developmental trajectories. Third, the use of a single set of frequency band boundaries for all age groups, as discussed above, may have limited the sensitivity of the alpha-band analysis. Finally, the NBS approach identifies subnetworks at the sensor level, and source-level analysis would be required to make more precise anatomical inferences about the cortical regions involved [24]. In addition, individual differences in

academic performance and baseline cognitive abilities within each age group were not explicitly controlled for and may contribute to the observed variability in connectivity and behavioral measures.

5 Conclusions

Our study demonstrates that age-related differences in EEG functional connectivity during visual search in school-age children are frequency-specific: theta-band connectivity reflects large-scale interhemispheric integration, whereas beta-band connectivity emphasizes localized intrahemispheric coordination. In both frequency bands, the most pronounced increase in connectivity strength occurred between Group 1 and Group 2, mirroring the behavioral improvement in reaction time. Importantly, linear mixed-effects modeling showed that connectivity within the identified subnetworks predicted visual search speed beyond the effects of age and task complexity, suggesting that the maturation of these networks constitutes a neural mechanism underlying developmental gains in search efficiency. These findings contribute to the understanding of how brain network reorganization supports cognitive development and may inform the design of neuroadaptive systems for assessing cognitive abilities in educational settings.

Availability of data and materials The data presented in this study are available on request from the corresponding author.

References

1. M.S. Thomas, D. Ansari, V.C. Knowland, Annual research review: educational neuroscience: progress and prospects. J. Child Psychol. Psychiatry **60**(4), 477–492 (2019)
2. S.D. Mayes, S.L. Calhoun, E.O. Bixler, D.N. Zimmerman, IQ and neuropsychological predictors of academic achievement. Learn. Individ. Differ. **19**(2), 238–241 (2009)
3. A. Cortés Pascual, N. Moyano Muñoz, A. Quílez Robres, The relationship between executive functions and academic performance in primary education: review and meta-analysis. Front. Psychol. **10**, 449759 (2019)
4. T. Moore, M. Zirnsak, Neural mechanisms of selective visual attention. Annu. Rev. Psychol. **68**, 47–72 (2017)
5. M. Quiroga, J. Santacreu, Is there a developmental gap in visual search for children with reported attention problems? J. Appl. Dev. Psychol. **56**, 42–51 (2018)
6. V. Antipov, Dynamics of oculomotor patterns during prolonged visual processing. Eur. Phys. J. Spec. Top. **234**(15), 4357–4364 (2025)
7. J.D. Cohen, *Cognitive Control: Core Constructs and Current Considerations. The Wiley Handbook of Cognitive Control* (Wiley, Chichester, 2017), pp. 1–28
8. C. Blair, Executive function and early childhood education. Curr. Opin. Behav. Sci. **10**, 102–107 (2016)
9. J. Guo, X. Luo, Y. Kong, B. Li, B. Si, L. Sun et al., Abnormal reactivity of brain oscillations to visual search target in children with attention-deficit/hyperactivity disorder. Biol. Psychiatry: Cogn. Neurosci. Neuroimaging **8**(5), 522–530 (2023)
10. M.D. Lewis, Self-organizing individual differences in brain development. Dev. Rev. **25**(3–4), 252–277 (2005)
11. M. Boersma, D.J. Smit, H.M. de Bie, G.C.M. Van Baal, D.I. Boomsma, E.J. de Geus et al., Network analysis of resting state EEG in the developing young brain: structure comes with maturation. Hum. Brain Mapp. **32**(3), 413–425 (2011)
12. F. Battiston, G. Cencetti, I. Iacopini, V. Latora, M. Lucas, A. Patania et al., Networks beyond pairwise interactions: structure and dynamics. Phys. Rep. **874**, 1–92 (2020)
13. R. Herzog, F.E. Rosas, R. Whelan, S. Fittipaldi, H. Santamaria-Garcia, J. Cruzat et al., Genuine high-order interactions in brain networks and neurodegeneration. Neurobiol. Dis. **175**, 105918 (2022)
14. S.A. Kurkin, A.N. Pisarchik, L.A. Mayorova, A.E. Hramov, Evolution of methods for assessing fMRI-based functional networks: from classical pairwise connectivity to higher-order interactions. Phys. Rep. **1174**, 1–66 (2026)
15. O.E. Karpov, E.N. Pitsik, S.A. Kurkin, V.A. Maksimenko, A.V. Gusev, N.N. Shusharina et al., Analysis of publication activity and research trends in the field of AI medical applications: network approach. Int. J. Environ. Res. Public Health **20**(7), 5335 (2023)
16. E. Combrisson, R. Basanisi, M. Neri, G. Auzias, G. Petri, D. Marinazzo et al., Higher-order and distributed synergistic functional interactions encode information gain in goal-directed learning. Nat. Commun. **16**(1), 7179 (2025)
17. J. Xu, B. Zhong, Review on portable EEG technology in educational research. Comput. Hum. Behav. **81**, 340–349 (2018)
18. C. Orovas, T. Sapounidis, C. Volioti, E. Keramopoulos, EEG in education: a scoping review of hardware, software, and methodological aspects. Sensors **25**(1), 182 (2024)
19. D. Cellier, J. Riddle, I. Petersen, K. Hwang, The development of theta and alpha neural oscillations from ages 3 to 24 years. Dev. Cogn. Neurosci. **50**, 100969 (2021)

20. M. McSweeney, S. Morales, E.A. Valadez, G.A. Buzzell, L. Yoder, W.P. Fifer et al., Age-related trends in aperiodic EEG activity and alpha oscillations during early- to middle-childhood. Neuroimage **269**, 119925 (2023)
21. E. Tan, S.V. Troller-Renfree, S. Morales, G.A. Buzzell, M. McSweeney, M. Antúnez et al., Theta activity and cognitive functioning: integrating evidence from resting-state and task-related developmental electroencephalography (EEG) research. Dev. Cogn. Neurosci. **67**, 101404 (2024)
22. S. Huo, J. Wang, T.K. Lam, B.W. Wong, K.C. Wu, J. Mo et al., Development of EEG alpha and theta oscillations in the maintenance stage of working memory. Biol. Psychol. **191**, 108824 (2024)
23. S. Bhavnani, G. Lockwood Estrin, R. Haartsen, S.K. Jensen, T. Gliga, V. Patel et al., EEG signatures of cognitive and social development of preschool children—a systematic review. PLoS ONE **16**(2), e0247223 (2021)
24. A.E. Hramov, V.A. Maksimenko, A.N. Pisarchik, Physical principles of brain–computer interfaces and their applications for rehabilitation, robotics and control of human brain states. Phys. Rep. **918**, 1–133 (2021)
25. V.A. Maksimenko, N.S. Frolov, A.E. Hramov, A.E. Runnova, V.V. Grubov, J. Kurths et al., Neural interactions in a spatially-distributed cortical network during perceptual decision-making. Front. Behav. Neurosci. **13**, 220 (2019)
26. R.J. Barry, A.R. Clarke, R. McCarthy, M. Selikowitz, S.J. Johnstone, J.A. Rushby, Age and gender effects in EEG coherence: I. Developmental trends in normal children. Clin. Neurophysiol. **115**(10), 2252–2258 (2004)
27. P.J. Uhlhaas, F. Roux, W. Singer, C. Haenschel, R. Sireteanu, E. Rodriguez, The development of neural synchrony reflects late maturation and restructuring of functional networks in humans. Proc. Natl. Acad. Sci. **106**(24), 9866–9871 (2009)
28. J. Kang, W. Mao, J. Wu, X. Huang, M.F. Casanova, E.M. Sokhadze et al., Development of EEG connectivity from preschool to school-age children. Front. Neurosci. **17**, 1277786 (2024)
29. J. Ramos-Loyo, P.V. Olguín-Rodríguez, S.E. Espinosa-Denenea, L.A. Llamas-Alonso, S. Rivera-Tello, M.F. Müller, EEG functional brain connectivity strengthens with age during attentional processing to faces in children. Front. Netw. Physiol. **2**, 890906 (2022)
30. V. Antipov, V. Grubov, T. Bukina, M. Khramova, Brain functional connectivity in sensory perception: fNIRS study, in *2025 9th Scientific School Dynamics of Complex Networks and their Applications (DCNA)* (IEEE, 2025), pp. 9–12
31. G. Nolte, O. Bai, L. Wheaton, Z. Mari, S. Vorbach, M. Hallett, Identifying true brain interaction from EEG data using the imaginary part of coherency. Clin. Neurophysiol. **115**(10), 2292–2307 (2004)
32. L. García Domínguez, J. Stieben, J.L. Pérez Velázquez, S. Shanker, The imaginary part of coherency in autism: differences in cortical functional connectivity in preschool children. PLoS ONE **8**(10), e75941 (2013)
33. S. Kurkin, N. Smirnov, E. Pitsik, M.S. Kabir, O. Martynova, O. Sysoeva et al., Features of the resting-state functional brain network of children with autism spectrum disorder: EEG source-level analysis. Eur. Phys. J. Spec. Top. **232**(5), 683–693 (2023)
34. E. Pitsik, S. Kurkin, O. Martynova, G. Portnova, A.E. Hramov, Hypergraph representation of multilayer brain network enhances autism spectrum disorder detection. Chaos: Interdiscip. J. Nonlinear Sci. **35**(7), 071104 (2025)
35. J.M. Sanchez Bornot, K. Wong-Lin, A.L. Ahmad, G. Prasad, Robust EEG/MEG based functional connectivity with the envelope of the imaginary coherence: sensor space analysis. Brain Topogr. **31**(6), 895–916 (2018)
36. V.V. Grubov, M.V. Khramova, S. Goman, A.A. Badarin, S.A. Kurkin, D.A. Andrikov et al., Open-loop neuroadaptive system for enhancing student's cognitive abilities in learning. IEEE Access **12**, 49034–49049 (2024)
37. A. Gramfort, M. Luessi, E. Larson, D.A. Engemann, D. Strohmeier, C. Brodbeck et al., MEG and EEG data analysis with MNE-Python. Front. Neuroinform. **7**, 267 (2013)
38. J. Iriarte, E. Urrestarazu, M. Valencia, M. Alegre, A. Malanda, C. Viteri et al., Independent component analysis as a tool to eliminate artifacts in EEG: a quantitative study. J. Clin. Neurophysiol. **20**(4), 249–257 (2003)
39. A.R. Clarke, R.J. Barry, R. McCarthy, M. Selikowitz, Age and sex effects in the EEG: development of the normal child. Clin. Neurophysiol. **112**(5), 806–814 (2001)
40. A. Zalesky, A. Fornito, E.T. Bullmore, Network-based statistic: identifying differences in brain networks. Neuroimage **53**(4), 1197–1207 (2010)
41. D. Bates, M. Mächler, B. Bolker, S. Walker, Fitting linear mixed-effects models using lme4. J. Stat. Softw. **67**, 1–48 (2015)
42. S. Lo, S. Andrews, To transform or not to transform: Using generalized linear mixed models to analyse reaction time data. Front. Psychol. **6**, 1171 (2015)
43. A. Badarin, N. Brusinskii, V. Grubov, T. Bukina, S. Kurkin, M.V. Khramova et al., Recurrency time entropy of brain wave rhythms as an indicator of performance on visual search tasks in schoolchildren. Eur. Phys. J. Spec. Top. **234**(15), 4899–4906 (2025)
44. J.F. Cavanagh, M.J. Frank, Frontal theta as a mechanism for cognitive control. Trends Cogn. Sci. **18**(8), 414–421 (2014)
45. J. Eisma, E. Rawls, S. Long, R. Mach, C. Lamm, Frontal midline theta differentiates separate cognitive control strategies while still generalizing the need for cognitive control. Sci. Rep. **11**(1), 14641 (2021)
46. C.G. Richter, W.H. Thompson, C.A. Bosman, P. Fries, Top-down beta enhances bottom-up gamma. J. Neurosci. **37**(28), 6698–6711 (2017)
47. G. Michalareas, J. Vezoli, S. Van Pelt, J.M. Schoffelen, H. Kennedy, P. Fries, Alpha-beta and gamma rhythms subserve feedback and feedforward influences among human visual cortical areas. Neuron **89**(2), 384–397 (2016)
48. A.K. Engel, P. Fries, Beta-band oscillations—signalling the status quo? Curr. Opin. Neurobiol. **20**(2), 156–165 (2010)
49. W. Klimesch, Alpha-band oscillations, attention, and controlled access to stored information. Trends Cogn. Sci. **16**(12), 606–617 (2012)

50. A.T. Hill, G.M. Clark, F.J. Bigelow, J.A. Lum, P.G. Enticott, Periodic and aperiodic neural activity displays age-dependent changes across early-to-middle childhood. Dev. Cogn. Neurosci. **54**, 101076 (2022)
51. J. Bathelt, H. O'Reilly, J.D. Clayden, J.H. Cross, M. de Haan, Functional brain network organisation of children between 2 and 5 years derived from reconstructed activity of cortical sources of high-density EEG recordings. Neuroimage **82**, 595–604 (2013)

Springer Nature or its licensor (e.g. a society or other partner) holds exclusive rights to this article under a publishing agreement with the author(s) or other rightsholder(s); author self-archiving of the accepted manuscript version of this article is solely governed by the terms of such publishing agreement and applicable law.